Article

J. Mex. Chem. Soc. **2021**, *65*(1)
Special Issue

ISSN-e 2594-0317

Mechanical Alloying: an Alternative Method to Produce NiMoW HDS Catalysts

R. Huirache-Acuña[1*], G. Alonso-Núñez[2], A. Vázquez-Guerrero[1], R. Martínez-Sánchez[3]

[1]Facultad de Ingeniería Química, Universidad Michoacana de San Nicolás de Hidalgo, Ciudad Universitaria, Morelia, 58060, México.
[2]Centro de Nanociencias y Nanotecnología-UNAM, Km. 107 Carretera Tijuana-Ensenada, CP. 22800, Ensenada, B.C. México.
[3]Centro de Investigación en Materiales Avanzados (CIMAV), Miguel de Cervantes No.120, C.P. 31109, Chihuahua, Chih., México.

***Corresponding author:** R. Huirache-Acuña, email rafael_huirache@yahoo.it.

Received July 24th, 2020; Accepted November 4th, 2020.

DOI: http://dx.doi.org/10.29356/jmcs.v65i1.1277

Abstract. In this work, quaternary alloys of Ni-Mo-W-Al were prepared by mechanical alloying. In addition, a process of chemical extraction by alkaline leaching was applied to remove aluminum in order to increase the specific surface area (SSA) and to generate porous materials, which were tested in the dibenzothiophene (DBT) hydrodesulfurization (HDS) reaction to determine their catalytic activity and selectivity. This study reveals the impact of the surface and structural modification of quaternary alloys on the catalyst performance and serves as well, as guidance for the design of novel HDS catalysts.
Keywords: Alloys; mechanical alloying; hydrodesulfurization; catalysts.

Resumen. En este trabajo, se prepararon mediante aleado mecánico aleaciones cuaternarias de Ni-Mo-W-Al. Adicionalmente, un proceso de extracción química mediante lixiviación alcalina se aplicó para eliminar aluminio con la finalidad de incrementar el área específica y generar materiales porosos, los cuales fueron activados y evaluados en la reacción de hidrodesulfuración (HDS) de dibenzotiofeno (DBT) para determinar su actividad catalítica y selectividad. Este estudio revela el impacto de la modificación estructural y superficial de las aleaciones cuaternarias sobre el comportamiento de los catalizadores y sirve como guía, además, para el diseño de nuevos catalizadores para HDS.
Palabras clave: Aleaciones; aleado mecánico; hidrodesulfuración; catalizadores.

Introduction

The increased demand for fossil fuels is a result of the continuing increase in population, especially in developing countries where energy options are limited, and the global interest in offsetting and/or eliminating the effects of burning these fossil fuels highlights the severity in consequence of large-scale industrial and automobile emissions [1]. To fulfill this increasing demand, the refineries must process heavier petroleum fractions feedstocks [2]. Nowadays, most of the refineries are not prepared to process heavy fractions and treating them represents a major operational and economic challenge for this industry. [3]

J. Mex. Chem. Soc. **2021**, *65*(1)
Special Issue

ISSN-e 2594-0317

Traditionally, sulfur has been removed from petroleum-derived feedstocks by a hydrodesulfurization (HDS) process using alumina-supported Mo or W catalysts promoted by Co or Ni. However, to satisfy new stringent environmental restrictions on the sulfur content of fuels, the refining industry is calling for more active HDS catalysts. New generations of catalysts, such as NEBULA®, are based on a totally different concept of bulk-like materials [4]. In this sense, research on unsupported NiMoW ternary systems has shown that those catalysts record an HDS activity fourfold greater than that of supported NiMo and NiW catalysts commercially available today. [5]

Unsupported HDS catalysts have been prepared by different methods, including comaceration [6], homogeneous sulfide precipitation [7], and thiosalt decomposition [8]. In these preparation methods, catalysts need to be activated under a H_2/H_2S mixture before being active in the catalytic reactions.

Mechanical alloying (MA) has not been quite explored as an alternative method. By using MA it has been possible to synthesize novel materials with special physical and chemical properties [9]. Preparation of Raney-type catalyst combines powders metallurgy routes with chemical treatments to obtain a highly porous final product [10]. Following the same principle, we applied the process of leaching to a quaternary alloy of Ni-Mo-W-Al prepared by MA, to remove the Al in order to increase its surface area and to explore the effect on the catalytic activity and selectivity of these nanocrystalline and porous NiMoW-Al. Catalysts were tested in the HDS of DBT performed in a batch reactor at 623 K and a total pressure of 3.1 MPa. DBT was selected as a model molecule, being this is a typical sulfur-containing compound present in the petroleum fraction of high-boiling point and coal derived liquids. [11]

Experimental

Catalyst synthesis

In a typical synthesis, Ni (99.8 % pure, -300 mesh in size), Mo (99.9 %, -200 mesh), W (99.9 %, -200 mesh), and Al (99.5 %, -325 mesh) crystalline metal powders were used as raw materials. Nominal composition was set to $(Ni_{50}Mo_{25}W_{25})_{50}Al_{50}$ at%. The mechanical alloying (MA) experimental runs were performed at room temperature in a commercial high-energy ball mill (Spex 8000). The milling time intervals were decided to be 9 and 50 h. The milling media to powder mass ratio was maintained constant at 5:1 for all experiments.

Due to the nature of AM, welding and fracture events occur during the process. To achieve a balance between these events, methanol was used as the process control agent (PCA) in all experiments. Devices and milling media (4.76 mm balls) used were made from stainless steel (SS). Static Ar atmosphere was selected during the milling process. In order to achieve a further increase on the surface area of samples the as-milled products were leached in an alkaline potassium hydroxide (KOH 20 % wt/wt.) solution at room (C) and refluxed temperature (H). Samples were labeled accordingly with the milling time (9 or 50 h), leaching time (1 or 2h) and temperature of alkaline solution (C or H).

Catalyst characterization

X-Ray Diffraction (XRD) characterization was performed in a Phillips XPert MPD Diffractometer equipped with a curve graphite monochromator with Cu Kα (λ = 0.154056 nm) radiation and XRD data were collected with a step mode of 0.05 ° with a collection time of 10 s/step operating at 43 kV and 30 mA. The specific surface area determination was made with a Quantachrome Nova 1000 series by nitrogen adsorption at 77 K using the BET isotherm. Samples were degassed under flowing argon at 473 K for 2 h before nitrogen adsorption. The mean standard deviation for surface area measurements was about 2 %. Transmission electron micrographs were obtained in a Philips TECNAI F20 FEG transmission electron microscope operated at 200 kV.

Catalytic activity and selectivity

The HDS of DBT has been extensively studied as a model reaction of petroleum feedstock [12]. Laboratory-scale studies have been performed in pressurized flow [13] and batch reactors [14]. By using batch reactors, useful information such as reaction rate constants (k) and selectivity (HYD/DDS) can be obtained by

J. Mex. Chem. Soc. **2021**, *65*(1)
Special Issue

ISSN-e 2594-0317

following the composition of the reaction mixture as a function of time. In this work, the HDS of DBT was carried out in a Parr model 4560 high-pressure batch reactor. The catalysts were not *ex-situ* sulfided to 400 °C under a flow of 15 % H_2S / 85 % H_2 gas 4 h before the HDS test (as in a typically synthesis). One gram of catalyst was placed in the reactor with a solution of 5 % vol of DBT in decaline. The reactor was then pressurized to 3.1 MPa with hydrogen and heated up to 623 K. After the working temperature was reached, sampling for chromatographic analysis was performed during the course of each run to determine conversion versus time dependence. The reaction time averaged was 5 h. The resulting products were analyzed using a Perkin-Elmer Clarus 500 gas chromatograph provided with an autosampler and a 10-ft long. 0.125 in. packed column containing 3 % OV-17 as separating phase on Chromosorb WAW 80/100. The main reaction products from the HDS of DBT are biphenyl (BP), cyclohexylbenzene (CHB) and tetrahydrodibenzothiophene (THDBT) (Fig. 1).

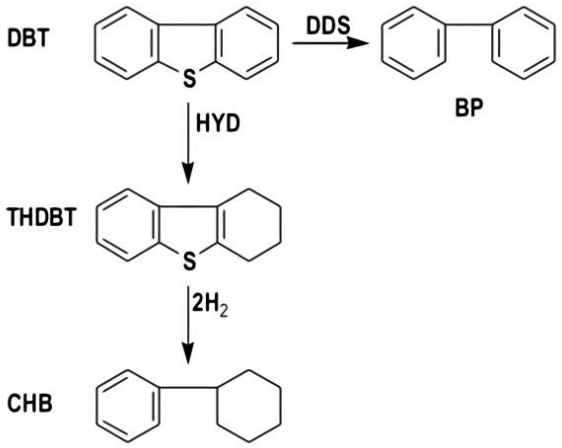

Fig. 1. HDS of DBT reaction scheme. DBT: dibenzothiophene; THDBT: tetrahydrodibenzothiophene; CHB: cyclohexylbenzene; BP: biphenyl HYD: hydrogenation reaction route; DDS: direct desulfurization reaction route.

Results and discussion

X-ray diffraction

The Fig. 2**a)** shows the XRD patterns obtained from powders produced by MA at 0, 9 and 50 h of milling time using a commercial high-energy ball mill (Spex 8000). It can be observed the presence of sharp peaks corresponding to nickel, molybdenum, tungsten and aluminum at 0 h of milling time. The most intense peaks at 2θ = 38.473 corresponds to (111) planes for aluminum (JCPDS-ICDD 4-787), at 2θ = 40.265 for (110) planes of tungsten (JCPDS-ICDD 4-806), at 2θ = 40.516 for (110) planes of molybdenum (JCPDS-ICDD 42-1120), and at 2θ = 44.508 for (111) planes of nickel (JCPDS-ICDD 4-850). From XRD pattern and JCPDS-ICDD cards, is reported that Aluminum and Nickel present face centered cubic (FCC) structure, and Molybdenum and Tungsten present body centered cubic structure (BCC). After 9 and 50 h of milling time, the peaks are broader and shorter, indicating the presence of a nanocrystalline structure. Signal from Al disappears after 9 h of milling time, remaining only signals from Mo, W and Ni. There is no evidence of formation of a new phase during milling, however clear evidence of a Mo and Ni signal shift was observed. Considering that the purpose of leaching was to eliminate aluminum from the quaternary NiMoWAl alloy so that the specific surface area could be enlarged. In this Fig. 2**b)**, XRD patterns obtained from leached samples; reveals that the elimination of aluminum during the chemical treatment apparently did not have a direct effect in the microstructural evolution. After leaching, nickel, molybdenum and tungsten corresponding peaks were further broadened and shortened, but these looked a little sharper. Remaining aluminum was not detected by XRD,

J. Mex. Chem. Soc. **2021**, *65*(1)
Special Issue

ISSN-e 2594-0317

probably because it is still in solution within Ni, Mo or W cell, in accordance with the typical peaks reflections shifting. On the other hand, W, Mo and Ni, retain their crystalline structure after leaching process, which is not in agree with Ivanov. [15]

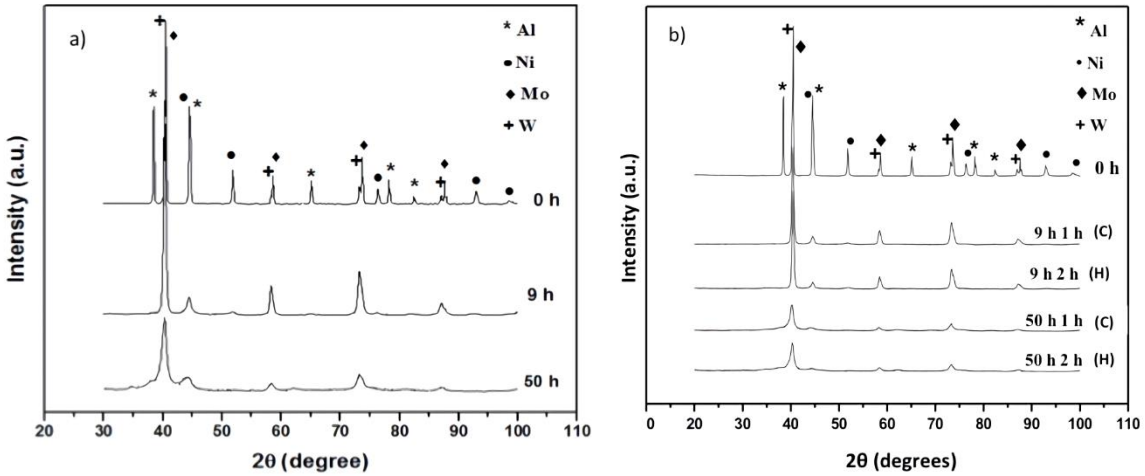

Fig. 2. XRD patterns for: **a)** milled samples and **b)** leached samples.

Transmision electron microscopy (TEM)

An interesting behavior for Ni, Mo and W was observed in XRD, since the elements retained their face centered cubic (FCC) and body centered cubic (BCC) structures after the milling process and leaching treatment. As it was previously stated, after milling, it was not possible to detect the presence of aluminum by XRD. However, STEM elemental mapping by using Energy Dispersive Spectroscopy (EDS) analysis confirmed the variation of aluminum content after the leaching process. Figures 3**a)** and **b)**, show elemental mapping from sample at 9 h of milling time (before leaching) and at 9 h of milling time and 2 h of leaching at boiling temperature, respectively. It is evident the presence of aluminum after the chemical extraction with KOH (not detected in XRD). However, it was observed that the aluminum amount decreased confirming that the chemical dissolution was selective for this element. The amount of aluminum removed depends on the milling time (Table 1), since a major amount of aluminum was possible to remove when a minor milling time was used (9 h). This phenomenon could be related with an effect of hindering of aluminum that decreased the diffusion of KOH and the dissolution of this element (for sample at 50 h of milling time) as was observed for I. Estrada-Guel *et al.* [16]. In the samples leached at boiling temperature (H) it was found the highest dissolution. For example, for 9h 1h (C) it was eliminated ~81.3% of the initial Al content whereas for 9h 2h (H) it almost reached ~88% of dissolution.

Table 1. Specific surface area and %Al removed after leaching.

Sample	Specific surface Area (m^2/g)±2	%Al removed[a]
9h	11	----
9h 1h (C)	51	81.3
9h 2h (H)	55	87.7
50 h	0.8	----
50 h 1h (C)	5	63.8
50 h 2h (H)	47	74.1

[a]%Al removed from STEM EDS analysis.

J. Mex. Chem. Soc. **2021**, *65*(1)
Special Issue

ISSN-e 2594-0317

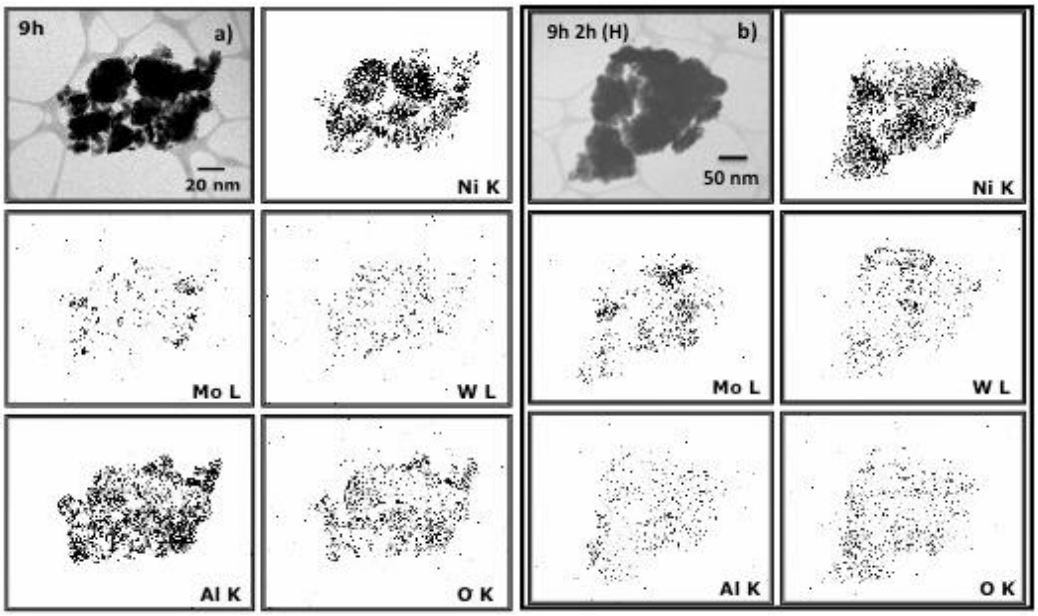

Fig. 3. STEM elemental mapping by EDS for samples: **a)** 9 h of milling time (before leaching), **b)** 9h of milling time and 2 h of leaching.

Fig. 4, shows the presence of nanocrystalline materials characteristic of the MA method. In addition, it was observed the presence of particles with "spongy" form and the formation of pores and cavities as a result of the chemical extraction of aluminum. On the other hand, Fig. 4**c)** shows the formation of defects produced during the milling process. The interplanar distance measured is very close to that corresponding to the (111) planes from nickel.

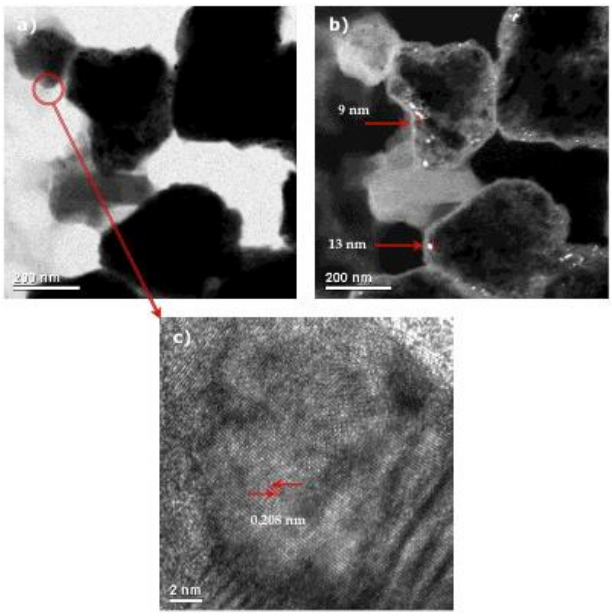

Fig. 4. TEM images from NiMoW Catalyst at 50 h of milling time and 1 h of leaching: **a)** Bright field, **b)** dark field, **c)** HRTEM.

J. Mex. Chem. Soc. **2021**, *65*(1)
Special Issue

ISSN-e 2594-0317

Textural properties

As seen in Figures 5**a)** and **b)**, all NiMoW samples exhibited type IV adsorption-desorption isotherms with an H_2 hysteresis loop in the partial pressure range from 0.4 P/P_0, characteristic of mesoporous materials [17]. BET specific surface areas present substantial variations with the chemical extraction process. This result shows that modifying the structure of quaternary alloys by removing Al (at least in the relative range of this study) influences the final textural properties achieved (Table 1). The specific surface area for the catalysts has an important effect in their catalytic activity. Likewise, larger surface area means a higher reaction area available, which is a factor that might favor the activity in the HDS reaction of DBT from the above results it is observed that as leaching time is increased, specific area values increase as well. The specific areas of the catalysts follow the trend: 9 h 2 h (H) (55 m^2/g) > 9 h 1 h (C) (51 m^2/g) > 50 h 2 h (H) (47 m^2/g) > 50h 1 h (C) (5 m^2/g). It was evident the increase in specific area from sample at 50 h of milling time (0.8 m^2/g) compared with that obtained after the leaching treatment at refluxed temperature: 50h 2h (H) (47 m^2/g). The lowest specific surface area from sample at 50 h might be related to with a major amount of welding and fracture events produced during the MA process.

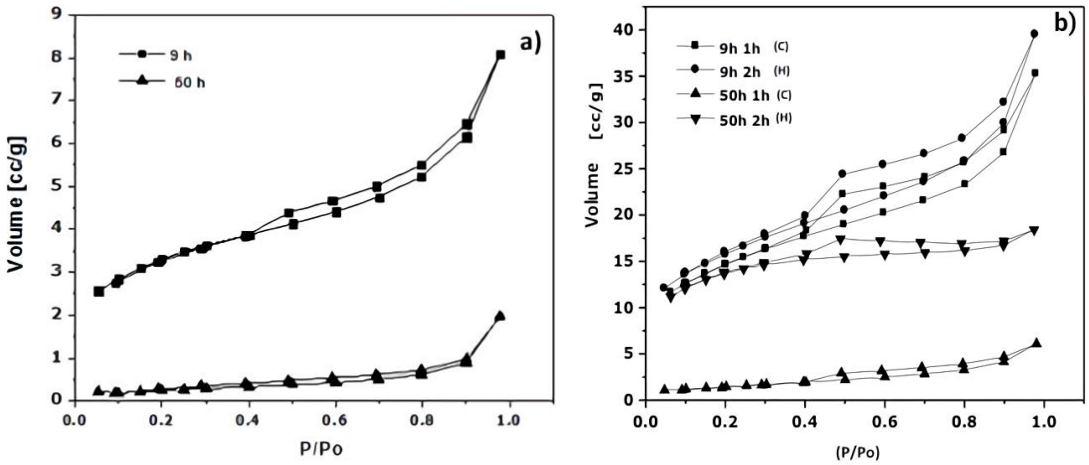

Fig. 5. N_2 adsorption-desorption isotherms of NiMoW Catalysts: **a)** before leaching, **b)** after leaching.

Catalytic activity

In this article, the activities of NiMoW catalysts, prepared by the MA method in the hydrodesulfurization (HDS) of dibenzothiophene (DBT) are reported. This reaction was selected for the following reasons: (i) DBT is a more refractory S-containing molecule than thiophene; (ii) it is a large S-containing molecule in which the sterical hindrance of the two phenyl groups may inhibit the accessibility to surface sites; and (iii) both HDS and hydrogenation functionalities can be simultaneously examined.

The pseudo first-order reaction rate constants (k) are displayed in Table 2. In addition, the DBT conversion follows the trend: 9h-2h (H) (21.2%) > 9h-1h (C) (18 %) > 50h-1h (C) (14.2%) > 50h-2h (H) (12.4%). Thus, considering the information from combined SSA and %Al removed (Table 1), the highest HDS activity of the 9h 2h (H) catalyst could be linked with its larger surface area and %Al removed after leaching. The %Al removed follows the trend: 9h 2h (H) (87.7%) > 9h 1h (C) (81.3 %) > 50h 2h (H) (74.1%) > 50h 1h (C) (63.8%). From Table 1, it is clear that aluminum removal improved the catalyst activity. In nanocrystalline alloys, the enormous quantity of available grain borders and the presence of inter-grain disorder can be important sources of active sites [18]. I. Estrada-Guel *et al.* [16] reported that apparently there was pulverization of particles during the Al dissolution for the NiMo-Al samples thus favoring the increasing of SSA.

J. Mex. Chem. Soc. **2021**, *65*(1)
Special Issue

ISSN-e 2594-0317

Table 2. Catalytic activity data for the HDS of DBT[a]

Catalyst	*k* (mol/g s)	% DBT Conversion	(HYD/DDS) sel. ratio[b]
9 h 1 h (C)	$3.4x10^{-7}$	18.0	0.46
9 h 2 h (H)	$3.7x10^{-7}$	21.2	0.5
50 h 1 h (C)	$2.3x10^{-7}$	12.4	0.4
50 h 2 h (H)	$2.5x10^{-7}$	14.2	0.5
NiMo/ γ-Al_2O_3[c]	$6.7x10^{-7}$	……	0.32

[a] HDS of DBT at *T*=350 ˚C; *P*=3.1 MPa; reaction time of 5 h; batch reactor.
[b] HYD/DDS ratio at 60 % of DBT conversion.
[c] From reference [22].

The HDS of DBT over the catalysts studied occurs through two parallel reaction pathways (Scheme 1): (i) hydrogenation (HYD) of one or two aromatic rings of DBT leading to the formation of intermediate THDBT and CHB, respectively; and (ii) direct desulfurization (DDS) route, which involves the hydrogenolysis of C-S with no hydrogenation of the aromatic rings (BP formation). In general, all catalysts synthesized in the present work (Table 2), present selectivity to generate BP, therefore the catalytic reaction follows the DDS pathway with HYD/DDS = 0.4-0.5 ratios. This indicates that in this particular case the preference for the HYD route linked with nickel was not observed [19]. However, the HDS *via* hydrogenation was slightly increased when boiling temperature (H) was used during the leaching process, showing the maximum value of the HYD/DDS ratio for the 9h 2h (H) and 50h 2h (H) samples. Considering this fact, one could assume that the HDS *via* hydrogenation might be related to the promotional effect of Ni species in the NiMoW catalyst and the DDS pathway could be linked with Mo and W species. However, Bataille *et al.* [20] studied the effect of Co or Ni promoter on the hydrodesulfurization of alkyldibenzothiophenes and concluded that DDS becomes the main pathway for the HDS of DBT since the hydrogenation of DBT into dihydrodibenzothiophene is the rate-limiting step for the two pathways. Kaluza *et al.* [21] reported that nickel for prepared mechanochemically NiMo/γ-Al_2O_3 catalysts promoted the direct desulfurization route of benzothiophene. On the other hand, a bimetallic reference from NiMo/γ-Al_2O_3 studied recently by us [22], showed a DDS pathway preference confirming the Ni promotion effect observed by Bataille *et al.* [20] and Kaluza *et al*. [21]. In addition, a higher catalytic activity was observed for NiMo/γ-Al_2O_3 catalyst reported in that work (See Table 2), since that sample was 1.8 times more active in comparison with the catalytic performance reported for 9h 2h (H) catalyst prepared by MA. Then, one might conclude that the addition of tungsten as the third metal to this catalytic system, decrease the performance of the MA synthesized catalysts. However, the synthesis conditions were very different in both systems and more studies should be made to elucidate this finding.

I. Estrada-Guel *et al.* [16] concluded that the activity of NiMo MA catalysts is due to both, the small particle size and the SSA values reached by leaching the aluminum. As observed in TEM (Fig. 4), a leached particle showed a very small crystal size (about 9 nm) with "spongy" form particles and the formation of nanopores and cavities. From these results it is possible to mention that nanocrystalline state is responsible of a high volume of grain boundary, and because this is a high-energy region it favors the surface phenomena like catalytic activity. This is an important finding of this research because it offers the possibility of preparing effective HDS catalysts by using MA.

Conclusion

NiMoW catalysts prepared with an alternative method of mechanical alloying were studied in the hydrodesulfurization of DBT under experimental conditions, which approach industrial practice. On the basis of the data presented aforementioned, the following conclusions can be drawn: (i), in general, the catalysts showed a removal of sulfur with DBT conversions from 12.4 to 21.2 %; (ii) the catalyst activity depends

J. Mex. Chem. Soc. **2021**, *65*(1)
Special Issue

ISSN-e 2594-0317

strongly on the % Al removed during the leaching alkaline process; (iii) all catalysts show a preference for the DDS pathway. The best catalyst response of 9 h 2 h (H) was linked to the increase of the specific surface area and a major percent of aluminum removed during the leaching process; (iv) the addition of tungsten as the third metal to this catalytic system, decrease the performance of the MA synthesized catalysts. This study reveals that a combined MA technique followed by a leaching process could be a promising method to produce HDS catalysts due to the synergized effect of small crystal size and presence of nanopores.

Acknowledgements

Dr. R. Huirache-Acuña wants to thank the support of CONACYT CIENCIA BASICA 182191 and CIC-UMSNH 2020 Projects (Mexico).

References

1. Tanimu, A.; Alhooshan, K. *Energy and Fuels* **2019**, *33*, 2810-2838. DOI: https://doi.org/10.1021/acs.energyfuels.9b00354
2. Díaz de León, J.N.; Ramesh Kumar, C.; Antúnez-García, J.; Fuentes-Moyado, S. *Catalysts* **2019**, 9, 87. DOI: https://doi.org/10.3390/catal9010087
3. Stanislaus, A.; Marafi, A.; Rana, M.S. *Catal. Today* **2010**, *153*, 1–68. DOI: https://doi.org/10.1016/j.cattod.2010.05.011
4. Plantenga, F.L.; Leliveld, R.G.; *Appl. Catal. A: Gen.* **2003**, 248, 1-7. DOI: https://doi.org/10.1016/S0926-860X(03)00133-9
5. Soled, S.L.; Miseo, S.; Krikak, R.; Vroman, H.; Ho, T.H.; Riley, K.L. US Patent 6, 299, 760 B1 2001.
6. Hagenbach, G.; Courty, Ph.; and Delmon, B. *J. Catal.* **1973**, 31, 264. DOI: https://doi.org/10.1016/0021-9517(73)90333-3
7. Candia, R.; Clausen, B. S.; and Topsøe, H. *J. Catal*. **1982**, 77, 564. DOI: https://doi.org/10.1016/0021-9517(82)90199-3
8. Zdrazil, M. *Catal. Today* **1988**, 3, 269. DOI: https://doi.org/10.1016/0920-5861(88)87051-2
9. Ivanov, E.; Makhlouf, A.A.; Sumiyama, K.; Yamauchi H.; Suzuki, K. *J. of Alloys and Compounds*, **1992**, 185, 25-34. DOI: https://doi.org/10.1016/0925-8388(92)90549-O
10. Yamashita, Hiromi; Yoshikawa, Masahito; Kaminade, Tadahiro; Funabiki, Takuzo; Yoshida, Satohiro. *Physical Chemistry in Condensed Phases*, **1986,** 82, No. 3, 707.
11. Huirache-Acuña, R.; Pawelec, B.; Rivera-Muñoz, E.M.; Guil-López, R.; Fierro J.L.G. *Fuel*, **2017,** 198, 145-158. DOI: http://dx.doi.org/10.1016/j.fuel.2016.09.042
12. Topsøe, H., Clausen, B. S., and Massoth, F. E., in "Catalysis, Science and Technology" (J.R. Anderson and M. Boudart, Eds.), vol. 11. Springer-Verlag, Berlin, **1996.**
13. Chianelli, R.R., and Pecoraro, T. A., U.S. Patent 4,508,847, 1985.
14. Jacobson, A. J.; Chianelli, R. R.; and Pecoraro, T. A. U.S. Patent 4,650,563, 1987.
15. Ivanov, E.; Makhlouf, A.A.; Sumiyama, K; Yamauchi, H. and Suzuki, K. J. of Alloys and Compounds, **1992**, 185, 25. DOI: https://doi.org/10.1016/0925-8388(92)90549-O
16. Estrada-Guel, I.; Alonso, G.; Ornelas, C.; Barajas-Villaruel, J.I.; Bejar-Gómez, L.; Espinosa-Magaña, F.; and Martínez-Sánchez, R. Journal of Metastable and Nanocrystalline Materials, **2004,** 20-21, 269-274. DOI: https://doi.org/10.4028/www.scientific.net/JMNM.20-21.269
17. Zhao, D.Y.; Huo, Q.S.; Feng, J.L.; Chmelka, B.F.; Stucky, G.D. J. Am. Chem. Soc. **1998**, 120, 6024–6036. DOI: https://doi.org/10.1021/ja974025i
18. Schulz, R.; Huot, J.Y.; Tradeu, M.L.; Dignard-Bailey, L.; Yan, Z.H.; Jin S.; Lamarre A.; Ghali E. and Van Neste A. J. Mater. Res., **1994**, 9 (11), 2998. DOI: https://doi.org/10.1557/JMR.1994.2998
19. Vrinat, M.; Lacroix, M.; Breysse, M.; Mosoni, L.; Roubin, M.; Catal. Lett., **1989**, 3 405-412. DOI: https://doi.org/10.1007/BF00771269

J. Mex. Chem. Soc. **2021**, *65*(1)
Special Issue

ISSN-e 2594-0317

20. Bataille, F.; Lemberton, J.L.; Michaud P., Péro, G.; Vrinat, M.; Lemaire, M.; Schulz, E.; Breysse, M.; Kasztelan, S. J. Catal. **2000**, 191, 409-422. DOI: https://doi.org/10.1006/jcat.1999.2790
21. Kaluža L.; Jirátová, K.; Tyuliev, G.; Gulková, D.; Balavanova, J.; Palcheva, R.; Kostejn, M.; Spojakina, A. *Reac. Kinetics, Mech. and Cat*. **2018**, 125, 319-337. DOI: https://doi.org/10.1007/s11144-018-1436-7
22. Huirache-Acuña, R.; Pérez-Ayala, E.; Cervantes-Gaxiola, M.E.; Alonso-Núñez, G.; Zepeda, T.A.; Rivera-Muñoz, E.M.; Pawelec, B. Catalysis Communications 2021, 148, 106162. DOI: https://doi.org/10.1016/j.catcom.2020.106162